SKIN DIGITAL MICROSCOPE IN COSMETIC LASER TREATMENT

Yuanli Yi*, Xiaofang Hong, Wentian Zeng, Jianhua Huang
Department of Orthopaedic Trauma, Huizhou Central People's Hospital, Huizhou 516001, Guangdong Province, China

ABSTRACT

Objective: *The development of medical laser technology began more than 40 years ago. Over the past 2 decades, this tool has become widely used in the field of laser cosmetology as a selective light treatment method. This article primarily studies the application effect of a skin digital microscope in cosmetic laser treatment.*

Methods: *In the experiment, a skin digital microscope was used to assist in clinical diagnosis, monitor the immediate response after laser treatment, and guide the clinic in choosing the most appropriate therapeutic dose. Algolab Photo Vector software was used to vectorize digital microscope photos of the skin, while CAD software was employed to measure photos in DXF format to obtain the area and circumference of target pores and scars before and after treatment. Lastly, the VivaScope 1500 system was used to perform RCM scanning on target skin lesion area or normal skin area.*

Results: *Using SAS statistical software, Wilcoxon's signed sequence and verification were performed before and after treatment; $P<0.05$ indicated a statistically significant difference. The experimental data showed 0.26% post-inflammatory pigmentation in patients with skin type 2.*

Conclusion: *The results reveal that the skin digital microscope provides an effective, objective, and quantitative method for the evaluation of treatment efficacy before and after treatment.*

Keywords: *Digital microscope, laser treatment, skin reaction, temperature control.*

DOI: 10.19193/0393-6384_2022_4_386

Received *March 15, 2021;* ***Accepted*** *March 20, 2022*

Introduction

The continuous progress of science and technology has led to the rapid development of laser technology. A laser's high brightness, monochromaticity, and directivity underlies this technological tool's penetration into various fields of science and technology as well as its current widespread use. Laser treatment can be employed in dealing with diseases that affect skin pigmentation, vascular diseases, hair loss, scarring, and more. A skin lesion image reveals the overlap of the contour and color of the sub-epidermal tissue structure, the main components of which are pigments and blood vessels. It is possible to use lighting and optical magnification devices to directly observe two-dimensional images from the horizontal plane of the skin. Therefore, many lesions that are not easily noticeable to the naked eye can be observed under dermoscopy. The skin digital microscope can collect clear images and analyze and process the images, greatly improving on the problems that hamper traditional microscopes, such as unclear imaging and slow image processing. In the diagnosis and treatment process, the skin digital microscope improves the accuracy of diagnosis with its sensitive,

fast, and non-invasive characteristics, especially when observing the regression of hemangioma, distinguishing hemangioma and port wine stains, and observing the thoroughness and effectiveness of the treatment of a pigmented nevus. Observe the curative effect before and after laser and guide the selection of laser parameters. According to Jahromi, recurrent aphthous stomatitis (RAS) is one of the most commonly seen lesions in the oral cavity. Due to its multifactorial nature, no definitive treatment for RAS currently exists. However, laser therapy has been recommended to reduce patient discomfort. The author's purpose was to evaluate the effects of low-level and high-level laser treatment on pain control and wound healing in RAS. In the study, 36 patients with mild RAS were divided into three groups. The first group (n=14) received CO2 laser treatment, while the second group (n=12) received InGaAlP diode laser treatment, and the third group (n=10) received fake laser treatment as a placebo. The researcher recorded each patient's pain severity before and after treatment, along with wound healing, patient satisfaction, and dysfunction before and after treatment. Although his research was practical, the factors considered were not comprehensive[1].

Song considered controlling surface wettability as critical to tribological behavior during friction and wear, especially in aqueous environments. Accordingly, the researcher used a fiber laser to process impregnated graphite to achieve a two-way wettability transition. He then used a scanning electron microscope to analyze the topography of the 3D confocal surface. Lastly, he used Raman spectroscopy and Fourier transform infrared (FTIR) spectroscopy to characterize the treated surface. He found that the surface treated with the low-energy laser became hydrophobic (the contact angle increased from 73.6° to 131.6°), while the surface treated with the high-energy laser became more hydrophilic (the contact angle decreased to 6.7°) Although this research is accurate, the research data are biased[2]. According to Huang, effective pain relief is essential to the health and satisfaction of skin patients receiving laser treatment. Therefore, the author investigated the potential results of using muscle relaxation techniques to reduce the pain of people who were having tattoos removed through laser treatment. The research subjects consisted of 56 participants (average age 18.1±2.1 years) who experienced muscle relaxation before receiving laser treatment. Peripheral skin temperature (PST) was measured at the beginning and end of the muscle relaxation period, after which the Baker Anxiety Scale was used to assess the level of anxiety. After the laser treatment was completed, a visual analog scale was used to measure the degree of pain. Although his research has certain reference value, it lacks specific research data[3]. Liu's goal was to explore the efficacy of non-incision venous laser therapy (EVLT) combined with hardened foam in the treatment of varicose veins of the lower extremities. A total of 140 patients (186 limbs) underwent laser surgery of the saphenous vein + injection sclerotherapy. The author recorded in detail preoperative information, intraoperative conditions, operation time, and hospital stay. During the 6-month follow-up, he found the closure of the main and branches of the great saphenous vein, postoperative pain, recovery of ulcers and dermatitis, and postoperative complications. Although his research has a clear direction, the operation steps have certain flaws[4].

This paper describes the use of a skin digital microscope to observe changes in the morphology, microstructure, physiological function, and metabolic process of cell tissues. The instrument can also dynamically scan and image human skin in real time with the mirror in real time, reaching the level of cell resolution, so as to understand various lasers. The real-time hotspot temperature and curve of the skin tissue heating image during the treatment revealed the relationship between the parameter settings and the complications in different types of laser treatment, providing a reference for the delineation of the safe treatment parameter range in the field of laser plastic surgery.

Methods

Skin digital microscope and laser treatment

Microscopic image processing

Because the entire point image distribution is equal to the product of the objective lens and the condenser lens point image distribution, a confocal system has a higher resolution than conventional microscopes. At the same time, due to the presence of the pinhole in the front of the detector, the confocal microscope also offers higher longitudinal resolution and higher contrast. The purpose of incorporating an image acquisition component into the microscope system is to make the resulting image available to more viewers, avoid the differences resulting from individual factors characterizing individual observation, and make the observation results more

objective. Early on, when film cameras were used for this purposes, film was used to capture images of objects under the microscope objective. Developing the film and fixing the image made it possible for more people to observe the scene under the microscope. However, this intermediate step was cumbersome, lengthening the time before an observation could be made. Moreover, one wrong step could lead to an unreliable or failed observation.

Record preservation was also problematic. Photographic information is stored by chemical agents and can degrade over time, causing an irrecoverable loss of information at some point. Therefore, once various electronic photosensitive devices (CCD and CMOS) were developed, they quickly replaced the original photosensitive film method of image storage, bringing about a revolutionary change in microscope use. As a result, microscopic observation has become more convenient, efficient, and interactive. Optical images are easier to store and share without worrying about a loss of information[5]. The image is the result of reflection and the projection of various objects using the energy of the light source. In essence, the imaging of the object by the photoreceptor represents the process of receiving light signals and converting them into electrical signals. Many kinds of sensors are involved, such as a single photosensitive element sensor, a strip sensor, or a sensor array.

In a broad sense, these sensors can be used to obtain images. Specifically, the term images refers to the two-dimensional images obtained by the sensor array. The stimulus received by the photosensitive element on the sensor is affected by many factors, expressed by the following formula:

$$I(x)=\int_{F}[S(\lambda)E(\lambda)R(x,\lambda)]d\lambda \quad (1)$$

In Equation (1), I is the photosensitive intensity on the xth pixel in the image, the integration limit F represents the range of the visible spectrum, S is the response factor of the imaging device, R is the spectral reflectance of the object surface, and E is the spectral distribution of the light source. The image received by the two-dimensional array is a single-channel grayscale image. For color images, three different channels are combined to express color information based on the principle of three colors. The general approach is to plate a different transmission film before each photosensitive element of the photoreceptor array to make it reflect the color information of each channel[6]. The formula is as follows:

$$\begin{cases} R(x)=k\int_{380}^{780}S_R(\lambda)E(\lambda)R(x,\lambda)d\lambda \\ G(x)=k\int_{380}^{780}S_G(\lambda)E(\lambda)R(x,\lambda)d\lambda \\ B(x)=k\int_{380}^{780}S_B(\lambda)E(\lambda)R(x,\lambda)d\lambda \end{cases} \quad (2)$$

The continuous wavelet transform is the first interpolation to restore, then calculate and solve. Interpolation technology is used to restore the original discrete signal into a continuous signal and then perform continuous wavelet transform according to different scales. For the dyadic wavelet transform, it is necessary to select the appropriate wavelet and filter. A spline dyadic wavelet can be used to meet the requirements. The discrete fast dyadic wavelet transform algorithm is directly applied to the original discrete digital signal to obtain the different scales. The wavelet coefficients. The former has no limitation on the choice of two-dimensional wavelet; it only needs the same two-dimensional smooth function to derive. In this way, under normal circumstances, there is no quick solution algorithm to overthrow the wavelet transform[7]. The specific expression is as follows:

$$\begin{cases} Mf(s,u,v)=\sqrt{\left|W^1f(s,u,v)\right|^2+\left|W^2f(s,u,v)\right|^2} \\ \tan Af(s,u,v)=\left(\dfrac{W^2f(s,u,v)}{W^1f(s,u,v)}\right) \end{cases} \quad (3)$$

Laplace operation is also a linear combination of partial differential operations, which is an isotropic (that is, rotation-invariant) linear operation. Using the difference instead of the derivative, the second-order partial derivative of the image function can be obtained as follows:

$$\frac{\partial^2 f(i,j)}{\partial x^2}=\Delta_x f(i+1,j)-\Delta_x f(i,j)=f(i+1,j)+f(i-1,j)-2f(i,j) \quad (4)$$

The Laplacian $\nabla^2 f$ is:

$$\nabla^2 f=\frac{\partial^2 f}{\partial x^2}+\frac{\partial^2 f}{\partial y^2}=f(i-1,j)+f(i+1,j)+f(i,j-1)-4f(i,j) \quad (5)$$

System structure of a skin digital microscope

The skin digital microscope can be used to obtain a stereoscopic image of an object. Before using high-resolution stereo images to operate, it is necessary to obtain accurate images from the focused stereomicroscope. In the same image, the brightness of different positions of the same image

is the same, and the image is focused at the same position. In other words, the value of the Tenengrad function of the two eye images at the same position is the same, and the range of image sequence numbers is the same. A skin digital microscope consists of an objective lens, a zoom system, a spectroscope, a prism, an eyepiece, a reflector, a camera interface, and more. On the left light path, the light of the observed object and other objects reaches the spectroscope after passing through the objective lens and zoom system. Part of the light passes through the spectroscope and then is magnified via the lens. After changing the direction of the prism, the light enters the left eyepiece, forming an enlarged virtual image in front of the human eye.

The other part is reflected by the spectroscope and then enters the left camera through the lens and reflector, forming a real image on the surface (target surface) of the photoelectric converter of the right camera. Similarly, on the right light path, part of the light of the scene enters the right eyepiece, forming an enlarged virtual image in front of the human eye, while the other part enters the right camera to form a real image on the target surface of the right camera. A zoom system is used to change the magnification of the stereomicroscope to capture the observed object as a whole or locally. In addition, the zoom system doubles the two optical paths at the same time[8].

Laser treatment

The laser primarily uses the photothermal effect, in which the laser interacts with biological tissues in cosmetic applications, such as laser skin rejuvenation, laser freckle removal, tattoo removal, and treatment of skin hemangioma. The volatile photothermal effect forms the basic principle of various laser beauty products today. The blue-black pigment in human skin tissue has a larger absorption coefficient for a 1064-nm laser, while red-brown pigment has a larger absorption coefficient for a 532-nm laser. A selective photothermal effect is possible because biological tissues have special absorption properties for incident photons, causing limited tissue damage in the target tissue.

Using the selective photothermal effect, a large amount of damage to tissue structure containing pigments is achieved by selecting a laser of a special wavelength to achieve a therapeutic effect. Utilizing the selective absorption of light and the biological stimulation of light, hemoglobin and water selectively absorb the laser energy, which then acts on the dermis of the skin, heating the collagen fibers in the dermis so that they contract and are denatured. Thus, the laser triggers a spontaneous wound-healing response in the dermal tissue. Additionally, collagen can be deposited in an orderly manner, increasing skin elasticity and reducing wrinkles[9-10].

The thermal damage that a laser inflicts primarily comes from the conduction of heat in the tissue, which is proportional to the action time. The longer the application time, the greater the range of thermal damage, even far beyond the scope of the tissue that the laser might directly vaporize. A familiar analogy from daily life serves as an illustration of the phenomenon: When an individual touches a very hot iron plate briefly with a finger, the skin will not be burned. However, longer contact between the finger and the iron plate will burn the skin. Most traditional lasers work in a continuous state in which the energy of the laser continuously acts on the tissue to cause heat accumulation and thermal damage. In contrast, pulsed lasers release high energy over a very short time, preventing effective heat conduction in the tissue and greatly reducing the degree of thermal damage[11-12].

Applying a skin digital microscope in cosmetic laser treatment

Subjects

We selected 68 cases of skin-related vascular disease and 80 cases of skin pigment-related disease. A skin digital microscope was used to make a clinical diagnosis, monitor the immediate response after laser treatment, and guide the clinic to choose the most appropriate therapeutic dose. All cases excluded relative contraindications and absolute contraindications before treatment. Relative contraindications included having received chemotherapy, skin radiotherapy, or chemical peeling (especially atrophic skin); smoking and diabetes; proliferative scars; active acne, abnormal pigmentation, or skin allergies; or high expectations for cosmetic treatment. Absolute contraindications included patients with systemic lupus erythematosus or skin sclerosis, severe scars, recent use of tretinoin, neurological or mental problems, inability to cooperate with postoperative care, or infectious disease.

Experimental equipment and main reagents

Equipment

595-nm pulsed dye laser, VivaScope 1500 system selection, CO2 dot matrix laser treatment instrument, skin digital microscope

Reagent

Distilled water, ultrasonic glue, lens cleaning paper, bonding window, tissue ring

Laser treatment plan

The dynamic cooling device was turned on during treatment. The target skin was irradiated only once during each treatment. Different pulse widths were used to treat different areas of the same patient's skin lesions, with the same energy density for each pulse width group during treatment. Four groups of different pulse widths were used to treat the skin lesions. In the corresponding area, purpura that appeared at the same time as the termination point were used to determine the energy density.

The interval between each treatment was one month, and the total treatment time was up to one month. If there were four groups of pulse widths, one group of skin lesions was cured, and a photographic and naked eye observation of the skin lesion color was made. As with normal skin, the trial treatment was considered to be terminated, and follow-up observation and corresponding evaluation were performed two months after surgery. Algolab Photo Vector software was used to vectorize the digital microscope photos of the skin (converting JPG format into DXF format), while CAD software was used to measure the photos in DXF format to obtain the area and circumference of the target pores and scar before and after treatment. Additionally, SAS statistical software was employed to process the data, while a Wilcoxon test was used to compare the levels before and after treatment, with $P<0.05$ considered a significant difference. An infusion pump was used to inject the photosensitizer into the vein at a constant speed within minutes. For intravenous bolus injection, a larger vein was chosen in the non-exposed part and the proper placement of the needle confirmed by injecting ml of normal saline before bolus injection to prevent the drug from leaking outside the blood vessel. After the drug infusion was completed, another 1 ml of saline was injected to reduce the drug concentration in the blood vessel and prevent photosensitivity.

The drug was shielded from all light during placement and injection to avoid any reduction in the effect of the drug. After injection of the drug, the subject was instructed to take measures to avoid sun exposure. The patient's normal skin was covered with adhesive tape and a double layer of red and black cloth. If the skin lesion and normal skin were intermingled and could not be covered, black marking pen was applied on the normal skin to protect the normal skin from damage. Hair removal at the treatment site was also performed to avoid affecting the illumination.

Skin digital microscope observation

We used the VivaScope 1500 system to perform RCM scanning on the target skin lesion area or normal skin area. The light source was an 830-nm laser beam, with the power less than 30 mW, a scanning offset range of 2.0 mm (XY horizontal direction), and a vertical resolution of 1.6 μm. We adopted a 30×water immersion objective lens, and the optical port was 0.9 NA. The accompanying dermatoscope had a resolution of $10^{\times}$, and the imaging range was an area 5 mm×5 mm in size. Dermoscopic images could be obtained because the thickness of the face and neck epidermis is generally not more than 50 μm when using RCM, while PWS skin lesions are abnormally expanded. The depth of the blood vessel was 100-1000 μm. The local skin was used to fix the tissue ring at the selected location with a sticking window, and the distilled water refractive index was used as the medium between the skin and the tissue ring to eliminate air bubbles to the greatest possible extent. Before scanning, we performed dermoscopic imaging, followed by confocal scanning imaging. Ultrasonic glue was used as the medium between the tissue ring and the lens.

The XY axis was a horizontal scan, while the Z axis was a sagittal plane scan, and the scale was recorded as depth. After positioning, we scanned each layer deeply and recorded the axis scale as the depth. Before the measurement of the facial skin, we thoroughly cleaned it to remove any residues of cosmetics and minimize the impact on the microscope imaging.

Statistical processing

We used Excel software to record and organize the data. SPSS 13.0 statistical software was used to perform variance analysis of compatible design in order to compare the differences between the average blood vessel diameter and the average blood vessel density of different pulse widths in the patient's skin lesions at the same scan level before and after treatment. Additionally, a paired test analysis was used to compare the patient's skin lesions. The difference in the average blood vessel diameter and blood vessel density was measured before and after treatment in the same pulse width group at different scan levels. $P<0.05$ was defined as statistically significant.

Results

Analysis of the application effect of the skin digital microscope in cosmetic laser treatment

Results of cosmetic laser treatment

When a laser irradiates the skin or mucosal tissues, four main interactions occur: reflection, transmission, scattering, and absorption. However, only the laser light absorbed by the tissue can play a therapeutic role. In human tissues, different target chromophores absorb different laser wavelengths. These target chromophores are primarily composed of hemoglobin, melanin, and water.

Therefore, using the appropriate laser wavelength to irradiate the corresponding tissue, along with considering the specific absorption of the target chromophore to affect the specific tissue, can achieve the treatment aim.

The mechanism of laser action is now considered to be as follows: After the target color base absorbs the laser, thermal effects affect the surrounding tissues, including pressure effects, electromagnetic effects, and biological stimulation effects. The heat generated by the tissue will diffuse to the surrounding tissues, a process called thermal relaxation.

The term thermal relaxation time refers to the time required for the color-based temperature to drop to half of its original value. Hence, the thermal effect of the laser on the target tissue depends on the temperature, duration, and thermal relaxation time of the target tissue, which are related to the wavelength, energy density, point, pulse width, frequency, and action time of the laser.

Table 1 and Figure 1 present a comparison between the complication group and the non-complication group. In the case of complications, the skin color of patients with complications was usually darker than that of patients without complications. This outcome is a more obvious phenomenon of post-inflammatory pigmentation. According to data comparison, 0.26% of patients with skin type 2 developed post-inflammatory pigmentation, while type 3, type 4, and type 5 skin patients had 2.6%, 11.6%, and 33%, respectively.

A comparison of the combination of complications and the data for the non-complication group shows no obvious correlation between the complication group and the non-complication group regarding gender, preoperative diagnosis, or laser parameters.

	Complication group	Non-complication group	P test	Total positivity
SPT	2.16	2.02	0.0017	82.87
MF (J/CM2)	25.50	25.10	0.48	36.73
ME (KJ)	4.19	4.20	0.9739	36.73
PFM	96.05	90.40	0.101	36.73
PM	3.95	9.60	0.101	36.73

Table 1: Comparison of complication group and non-complication group.

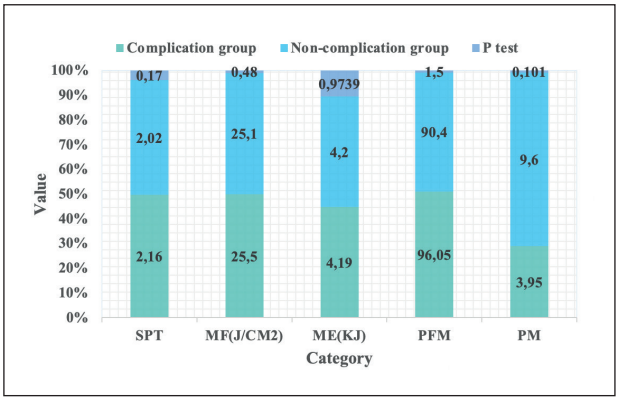

Figure 1: Comparison results of the complication group and the non-complication group.

Application effect of skin digital microscope

The dermoscopic pore wrinkles, scar area, and circumference values of 38 patients were measured before and after treatment via skin digital microscope data, as shown in Table 2 and Figure 2. The difference was tested for normality, W=0.915925, P<0.05. The difference value did not follow a normal distribution. According to the results of the SAS Wilcoxon signed-rank test, S=370.5, P<0.05, the difference before and after treatment was statistically significant.

A comparison of the detection rate of each index in the CLSM scan image and the pathological image of seborrheic keratosis revealed that CLSM had an effect on papilloma-like hyperplasia, spinous hypertrophy, hyperkeratosis, follicular horn plug, and horn cyst. In addition, the detection rate of 6 pathological indicators of superficial dermal inflammatory cell infiltration was not statistically significant compared with pathology, and the P values were all >0.05. CLSM demonstrated a high diagnostic coincidence rate between the detection rate of seborrheic keratosis and the pathological examination. The coincidence rates of each index were 87.2% of papilloma-like hyperplasia, 92.3% of spinous hypertrophy, 76.9% of hyperkeratosis, 74.3% of hair follicle horn plug, 87.2% of keratocyst, and 66.7% of superficial dermal inflammatory cell

infiltration, which can be seen. CLSM had a high diagnostic coincidence rate for papilloma-like hyperplasia, spinous hypertrophy, hyperkeratosis, follicular horn thrombus, and corner cyst but a slightly lower diagnostic coincidence rate for superficial dermal inflammatory cell infiltration.

Numbering	Average area		Average circumference	
	Before treatment	After treatment	Before treatment	After treatment
1	1.0634	0.7881	3.9518	2.3612
2	1.6270	0.9157	5.2054	3.5015
3	0.4093	0.1161	2.3598	1.2925
4	0.4198	0.1140	2.7746	2.1475
5	0.3781	0.1107	2.2171	1.2424
6	0.7830	0.3443	2.3131	1.9087
7	0.6187	0.3914	2.7741	1.8468
8	0.3310	0.1384	2.2565	1.2917
9	1.4827	0.7946	5.7125	3.9550
10	0.4532	0.1674	3.2385	1.7676
11	1.2923	0.7430	4.1779	3.1689
12	1.6298	0.8305	4.9197	3.0067
13	5.0627	3.1814	10.1995	6.6910

Table 2: Dermoscopic pore wrinkle and scar area and circumference values.

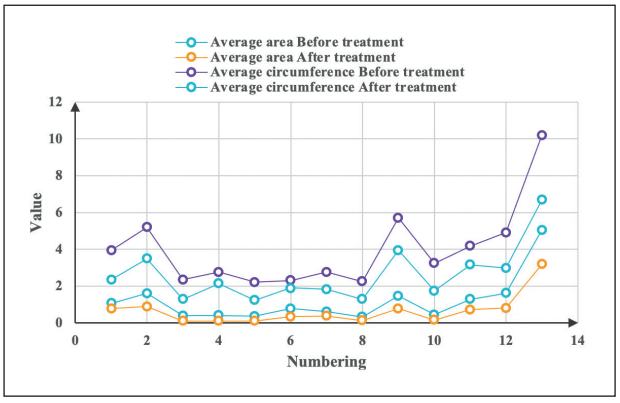

Figure 2: Dermoscopic pore wrinkle/scar area/circumference comparison.

After pulsed dye laser (PDL) treatment, the blood vessels in the skin of port wine stains exhibited only a purpura reaction under dermoscopic examination, indicating the most appropriate treatment dose.

Under dermoscopy, blood vessels that show obvious contraction and display a gray-white color may indicate blister scar side effects, while hemangioma presents a dense red appearance. After long-pulsed Nd:YAG 1064-nm laser treatment, the blood vessels were obviously contracted, and the skin was slightly white. Dermoscopy often provides more sensitive post-treatment response than the naked eye, which greatly reduces the risk in clinical treatment. Different pigmented diseases present different images under dermoscopy.

Specifically, epidermal pigmented diseases are black or brown, while dermal pigmented diseases appear gray or blue using this technology. For instance, following the treatment of coffee spots of epidermal pigmented diseases using a Q-switched Alexa 755-nm laser, an immediate response under dermoscopy showing slightly white pigmented spots indicates the best treatment dose.

In another example, after receiving laser treatment, patients with chloasma will show slightly reddened skin and white hair in the treatment area. These microscopic results and fine monitoring are conducive to better clinical treatment.

Image processing analysis

Figure 3 displays the effect of the signal-to-noise ratio on the image under static conditions. Because the microscope image is too large, the compression time is also very long.

Using JPEG or H.263 for intra-frame compression, it takes 2.4 seconds to compress a frame of a 1280×1024 image; meanwhile, JPEG-2000 takes longer. Because it cannot meet the system's 10fps requirement, other methods must be found for intra-frame compression. Obviously, the whole-pixel search does not represent the real motion vector because the displacement between frames in a video sequence is completely independent of the sampled lattice.

The sub-pixel search can supplement the accuracy of the whole-pixel search, thereby effectively reducing the error between the original frame and the predicted frame. For this reason, a half-pixel search and a full-pixel search form the motion estimation unit of H.263 and MPEG-4 standards. However, the fast search algorithm mainly focuses on the full-pixel search, and the half-pixel precision search usually adopts the full-search method, that is, searching all 8 half pixels obtained by linear interpolation around the whole pixel. With the continuous improvement of the whole-pixel search algorithm, when the size of the search area is 15×15, the traditional whole-pixel fast search algorithm can reduce the number of whole pixels to be searched for each block to less than 20.

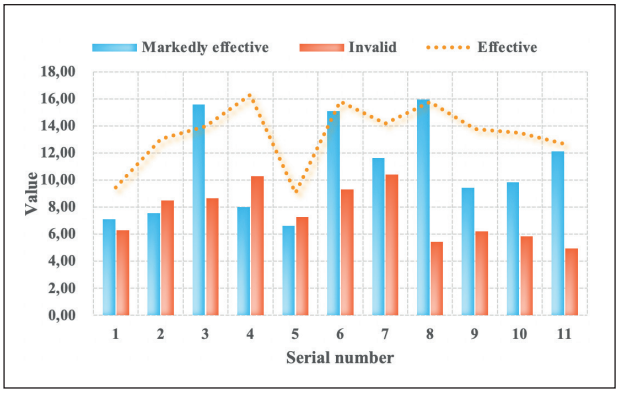

Figure 3: The result of image signal-to-noise ratio.

Effect of skin digital microscope in cosmetic laser treatment

Figure 4 illustrates a comparison of the efficiency of the feature-matching strategy with higher robustness. It can be seen that the total number of matches detected in the initial stage gradually increased with the enhancement of Gaussian noise, and the matching pairs retained after the feature-matching removal operation gradually decreased. Nevertheless, we successfully removed all errors through a four-step feature matching operation. Matched feature pairs can resist the interference caused by noise on the registration of multi-focus images. Dermoscopy image analysis technology can scientifically link the general clinical manifestations of dermatology with microscopic images of histopathology. Although the naked eye was mainly used to diagnose skin injuries in the past, wounds that do not require pathological biopsy or direct surgical resection sometimes occur.

Before confirming benign or malignant tumors, the scope of surgery may also be difficult to determine. In addition, checking all details related to the damage caused by multiple diseases is difficult. Dermoscopy has mainly been used in the diagnosis and differential diagnosis of pigmented diseases, such as pigmented moles and early-stage malignant melanoma, which has limited the indications to a certain extent. In the near-ultraviolet, visible, and near-infrared spectral regions, since the color of biological tissue has the characteristic of selective absorption of laser energy, it is necessary to understand the optical characteristics of the laser beam acting on the target area of the tissue. As previously mentioned, the laser radiation acting on the skin surface is typically reflected, absorbed, scattered, or transmitted by the skin. Of the laser (wavelength 300-1000 nm) radiation energy that penetrates the skin, 99% is absorbed by the 3.6 mm layer outside the tissue. The absorption process is not only related to tissue components (including biological pigments) but also relates to the scattering effect of the unevenness of the tissue structure. Studies have shown that the maximum and minimum reflections of the tissue to the laser are consistent with its minimum and maximum absorption, respectively. Therefore, the measurement of the reflection of the tissues to the laser in each band can determine the quantitative data related to entering the organism to a certain extent. The unique advantage of reflectometry is that it can be measured on living human skin. The reflection of electromagnetic radiation in the wavelength range of 400~1000 nm from tissues shows considerable differences related to the inherent pigment, blood flow, and blood volume.

Different vascular structures under dermoscopy reveal different shapes. Blood vessels with large diameters irregularly separate into many small capillaries in the branches. Because the position of the blood vessels is very superficial (under the epidermis), they appear bright red, such as spider nevi. Curved and unbranched blood vessels line the lesions, such as varicose veins in the legs. Small blood vessels (with a diameter of 0.01~0.02 mm) are arranged irregularly and densely, such as in the case of port wine stains and facial telangiectasia. Erythema reactions are common at the edges of degenerative lesions, such as the edges of dying hemangioma lesions. A combination of two or more types of blood vessels, such as arteriovenous malformations, port wine stains, etc.

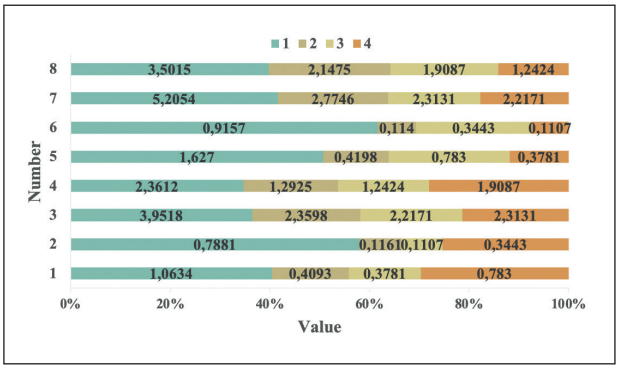

Figure 4: Results of a comparison of the efficiency of feature-matching strategies with higher robustness.

Discussion

This article provided an application effect analysis of the use of a skin digital microscope in cosmetic laser treatment. Dermoscopy, as a new, non-invasive dermatological examination method, is simple to operate, has a wide range of indications,

and offers a fast method of detection. It can largely compensate for the limitations of relying only on the naked eye for clinical observation and provides more information regarding microscopic skin lesion characteristics. Dermoscopic images are easy to collect and save, making it convenient to compare the development and changes of the lesions during long-term follow-up observation.

An electronic dermatoscope is a new technological tool that combines computer technology with a dermatoscope. Digital dermoscopy provides high-quality images, greatly facilitating the processing and measurement of dermoscopy images. Furthermore, the computer can store, search, and retrieve images conveniently and quickly.

Human skin tissue has the characteristic of selective absorption of light, an important principle that forms the basis of cosmetic treatments that employ laser technology. Selecting the appropriate laser wavelength for treatment according to the absorption wavelength of the target tissue is the key to laser cosmetic treatment that can effectively remove diseased skin tissue without damaging the surrounding normal skin tissue.

At present, laser cosmetology is widely used and has achieved good therapeutic effects on many diseases that are difficult to cure with conventional methods. This approach has gradually become an effective, practical treatment method, trusted by doctors and patients alike. Dermatoscopy can fully assist and guide the clinical diagnosis and differential diagnosis of skin tissues and other body surface mucosal lesions. Specifically, it is used to help determine clinically accurate laser treatment energy and observe the immediate tissue response. It has the advantages of more sensitivity and accuracy. Thus, this objective and effective method provides a new scope for exploration for the clinical application of a skin digital microscope.

This study used digital microscopic observation of the skin, combined with analysis of the clinical curative effect, to demonstrate the clear curative effectiveness of photodynamic therapy on port wine stains and proved that the observation results of the two are basically consistent. Therefore, a laser confocal microscope provides a more reliable method for clinical detection of port wine stains. Future research might explore the changes in blood vessels in port wine stains under different treatment methods, such as pulsed dye laser and photodynamic therapy under different parameters, so as to determine their impact on the therapeutic effect. This endeavor can provide a theoretical basis for clinical optimization of parameters and the selection of reasonable treatment plans, an outcome having considerable significance for clinicians and their patients.

References

1) Zeini Jahromi N, Ghapanchi J, Pourshahidi S, Zahed M, Ebrahimi H. Clinical Evaluation of High and Low-Level Laser Treatment (CO2vsInGaAlP Diode Laser) for Recurrent Aphthous Stomatitis. J Dent (Shiraz) 2017 Mar; 18(1): 17-23.
2) Lin YJ, Song H, Oh S, Voroslakos M, Kim K, et al. A 3.1-5.2GHz, Energy-Efficient Single Antenna, Cancellation-Free, Bitwise Time-Division Duplex Transceiver for High Channel Count Optogenetic Neural Interface. IEEE Trans Biomed Circuits Syst 2022 Jan 4; PP.
3) Huang F, Chou WJ, Chen TH, Chen C, Hsieh YL, et al. Muscle Relaxation for Individuals Having Tattoos Removed Through Laser Treatment: Possible Effects Regarding Anxiety and Pain. Lasers Med Sci 2016 Aug; 31(6): 1069-74.
4) Fresa M, El Ezzi O, DE Buys Roessingh A, Qanadli SD, Ney B, et al. Ultrasound-Guided Percutaneous Endovenous Laser Treatment Combined With Sclerotherapy for the Treatment of Large Intramuscular Venous Malformations. Int Angiol 2021 Feb; 40(1): 1-8.
5) Filippini M, Sozzi J, Farinelli M, Verdelli A. Effects of Fractional CO2 Laser Treatment on Patients Affected by Vulvar Lichen Sclerosus: A Prospective Study. Photobiomodul Photomed Laser Surg 2021 Dec; 39(12): 782-88.
6) Liu JJ, Fan LH, Xu DC, Li X, Dong ZH, et al. The Endovenous Laser Treatment for Patients With Varicose Veins. Pak J Med Sci 2016 Jan-Feb; 32(1): 55-8.
7) Ohshiro T, Ohshiro T, Sasaki K, Kishi K. Picosecond Pulse Duration Laser Treatment for Dermal Melanocytosis in Asians: A Retrospective Review. Laser Ther 2016 Jun 29; 25(2): 99-104.
8) Adebanjo GD, Kornilovitch P, Hague JP. Superlight Pairs in Face-Centred-Cubic Extended Hubbard Models With Strong Coulomb Repulsion. J Phys Condens Matter 2022 Jan 5.
9) Russo A, Turano R, Morescalchi F, Gambicorti E, Cancarini A, et al. Comparison of Half-Dose Photodynamic Therapy and 689 nm Laser Treatment in Eyes With Chronic Central Serous Chorioretinopathy. Graefes Arch Clin Exp Ophthalmol 2017 Jun; 255(6): 1141-48.

10) Dou W, Yang Q, Yin Y, Fan X, Qiu L, et al. A Randomized, Split-Face Controlled Trial on the Safety and Effects of Microneedle Fractional Radiofrequency and Fractional Erbium-Doped Glass 1,565-nm Laser Therapies for Baggy Lower Eyelids. J Cosmet Laser Ther 2021 Nov 23: 1-8.
11) Park JM, Tsao H, Tsao S. Combined Use of Intense Pulsed Light and Q-Switched Ruby Laser for Complex Dyspigmentation Among Asian Patients. Lasers Surg Med 2008 Feb; 40(2): 128-33.
12) Schaffer LR, Hubbard GB (III), Mukkamala K, Rao P. Atypical Late-Onset Exudative Retinal
13) Detachment in a Treatment-Naïve Infant With Retinopathy of Prematurity. Ophthalmic Surg Lasers Imaging Retina 2021 Jul; 52(7): 403-6.

Acknowledgement:
The Scientific Research Project of Health and Family Planning Commission of Hainan Province (No.18A200117).

Corresponding Author:
Yuanli Yi
No. 41 Erling North Road, Huicheng District, Huizhou City, Guangdong Province, China
Email: wwn74g@163.com
(China)